From MAMI to the Polytrons — Microtrons in the 10 GeV Range

Helmut Herminghaus
Im Bornacker 11
W 6531 Weiler/Bingen
Germany

Abstract

After some supplementary remarks on the construction of the cw microtron cascade MAMI, certain aspects of higher order microtrons as accelerators for up to about 30 GeV are communicated.

1 INTRODUCTION

Acceleration of electrons allows multiple use of a linac by recirculation because the particle velocity is constant in energy. For cw operation it is even required for economic reasons, no concern whether the linac is normal conducting or superconducting. Among the possible recirculation schemes, microtrons follow a peculiar philosophy in that, from one linac passage to the next, the beams of successive turns are shifted with respect to each other by an integer number ν of wavelengths λ ("resonance condition"; usually $\nu = 1$). This is achieved by the natural orbit length increase in the bending magnets, providing a longitudinal dispersion of the recirculation arc which is given by $\nu \cdot \lambda / \Delta E_c$, where ΔE_c is the energy gain in one revolution.

Non-isochronous recirculation generally results in a most beneficial output energy stabilisation. The special microtron philosophy allows an elegant method of longitudinal tune control, as will be shown later.

2 THE MAINZ MICROTRON "MAMI"

2.1 *General Philosophy*

The concept of MAMI is based on the use of normal conducting structure [1]. If normal conducting structure is to be used for acceleration close to 1 GeV in cw operation, a large number of recirculations has to be provided in order to improve the otherwise extremely poor efficiency. This is easiest done using the race track microtron (RTM) scheme. It would not be practical, however, to provide acceleration from a few MeV to 800 MeV in one single microtron: since the first return path should clear the linac, an unpractically large orbit diameter would result for the last turn. Rather, as a rule of thumb, the energy gain in a RTM should not exceed a factor of about 10. Thus MAMI is a cascade of three RTMs. This also makes possible the use of a very simple focusing scheme: quadrupoles are provided on the linac axis only (two singuletts in the first stage, two dupletts in stage two and three), acting on all orbits simultaneously. Due to the decrease of focusing strength, the Beta function increases about proportionally with energy. Thus, taking pseudo-damping into account, the beam size stays roughly constant during acceleration. Also, monitoring of beam position and intensity is done for all orbits simultaneously by rf cavities on either end of the linac, individual orbits being identified by the time at which a short beam intensity modulation passes the cavities. These informations are made available to the control computer (Microvax II) by means of a fast flash-ADC. Steering is done on each individual return path by two pairs of steerers each. Fig. 1 shows the final setup of MAMI, table 1 gives its main parameters. The emittance values given for

General				
Stage No.		I	II	III
Input energy	MeV	3.46	14.39	179.8
Output energy	MeV	14.39	179.8	855
No. of recirculations		18	51	90
Magnet system				
Magnet distance	m	1.67	5.60	12.86
Flux density	T	0.1028	0.5553	1.2842
Max. orbit diam.	m	0.97	2.17	4.43
Weight per magn.	to	1.3	43	450
Gap width	cm	6	7	10
RF System				
No. of klystrons		1	2	5
Linac length (el.)	m	0.80	3.55	8.87
rf power dissip.	kW	8	48	103
rf beam power	kW	1.1	17	68
Energy gain	MeV	0.6	3.24	7.5
Beam (100 μA)				
Energy width	keV	± 9	± 18	± 60
Emittance vert.	μm	$< .17\ \pi$	$< .014\ \pi$	$\leq .04\ \pi$
Emittance hori.	μm	$< .17\ \pi$	$< .014\ \pi$	$\leq .14\ \pi$
Injection:	100 keV gun and three linac sections, fed by another klystron			
Extraction:	from each even numbered return path of RTM 3, i.e. in steps of 15 MeV			
rf-structure:	on-axis-coupled biperiodic standing wave, vacuum brazed OFHC copper, beam aperture 14 mm diameter			
Klystrons:	Thomson TH 2075 50 kW cw max., 2449.6 MHz			

Table 1: Main Parameters of MAMI

the third stage need some comments: horizontal emittance is blown up by synchrotron radiation effects. The value given should contain 99,9% of the beam intensity. Vertical emittance should ideally be about 0.003 π·mm·mrad. The value given assumes that some emittance is transferred from the horizontal plane due to some accidental

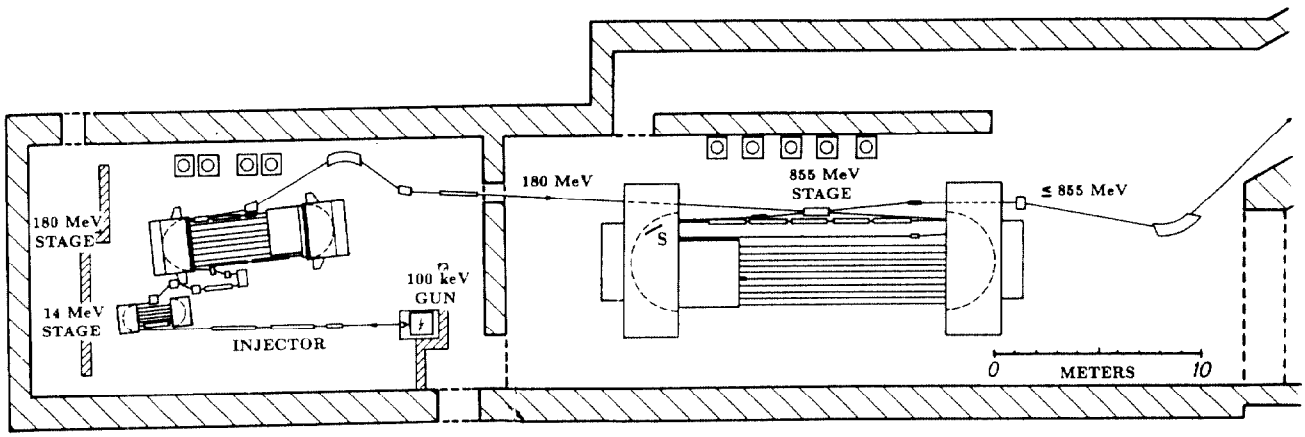

Figure 1: Final setup of MAMI

coupling.

2.2 Construction and Performance

During the years of construction the parameters given in [1] changed somewhat. For instance, the second stage was upgraded from 100 MeV to 180 MeV in order to allow experiments beyond the pion threshold before realisation of the third stage. This two-stage setup [2] was operated routinely from 1983 to '87 [4]. The final setup was set into operation in August 1990 [3]. A couple of details of this setup has been described earlier [5], [6], [7], [8], [9], [10], [11], [12]. Therefore, in this paper only some supplementary remarks are given. For further details see [13].

In the early days of design there were serious doubts whether the third stage with its many, rather weakly guided and relatively long recirculations could ever be operated safely. This, however, turned out to be not a problem at all: once the beam is injected properly, it is easily guided through all turns and it behaves stably for many hours. Generally, such a setting is closely reproducible from run to run. Some residual fine adjustment of the steerers may be done automatically by the control computer using the readouts of the position monitors. We assign the good performance of the third stage i.a. to the careful homogenizing of the reversing magnets by surface correcting coils. Details are described in [9], the result is shown in fig. 2. It turned out that the method may be applied rather successfully also in the fringe region outside the pole face area if the correcting current is just increased by a factor of about 2.5 above the value to be used inside the gap. This is surprising since the boundary conditions on which the method is based is heavily violated outside the gap.

Initially, there have been some beam position fluctuations and drifts at the output of the second stage. Both could be suppressed very effectively by simple mechanical means like reinforcing the magnet supports [13]. In fact, the wide span between input and output energy of the second stage makes it especially sensitive to angular position changes of the magnets with respect to each other.

Yet, some long term (several days) drift of the beam is still observed, which is assigned to slow deformations of the (relatively new) building. Such drifts, however, are well below the limits of the steering system and are easily corrected by computer control.

A most promising approach has been done to perform beam matching automatically by a neural network simulation program. This would be especially helpful for the beam transport system downstream MAMI which has to be operated with different settings depending on beam energy and user's demands.

The accelerator sections used in the injector linac and in the microtrons were operated without any problem so far. Nominal power level being 10 to 14 kW/m, they have also been operated with up to 20 kW/m over longer periods for testing. Even after being under air for several days, conditioning to full rf power takes one hour only.

There are, however, occasionally difficulties with two short, low powered sections, which serve for matching between the microtrons. Especially after longer intervals in operation they are susceptible to rf breakdowns together with vacuum interlocks - inspite of the low operation level of about 1 kW/m. This can be cured by conditioning at some higher level. The behaviour is not yet quite understood, but multipacting might play a dominant role.

Energy jitter can be detected very sensitively in a straigthforward manner by observing the jitter of the bunch phase advance from turn to turn. By that we find the output energy jitter to be $\leq 2 \cdot 10^{-5}$ bin at 855 MeV. This is compatible with the observed rf amplitude jitter of about $2 \cdot 10^{-3}$.

2.3 Limits of the race track microtron

The output energy of a RTM is limited to about 1 GeV for two reasons:

1. Magnet weight: for each energy range of a RTM there is an optimum value of flux density in the reversing magnets, which increases with energy. Once the saturation limit is reached, further increase of energy requires the magnet volume to grow roughly as the third power of energy.

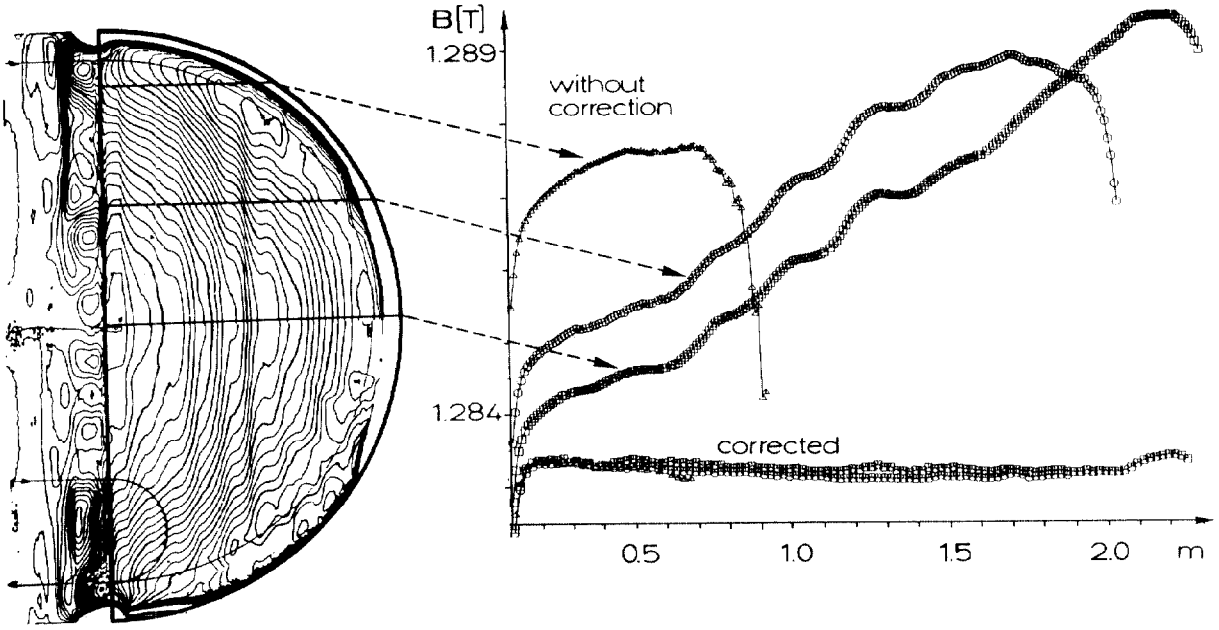

Figure 2: Homogenizing of a reversing magnet by surface correcting coils. Left: field map before correction (ΔB = 0.2 Tesla). Right: three cuts of the field map, before and after correction.

2. Horizontal emittance: its growth per revolution due to synchrotron radiation is given by

$$\Delta\varepsilon = \frac{55\pi^2}{12\sqrt{3}} \cdot \frac{r_e \hbar}{m_0 c R^2} \cdot \left(\frac{E}{m_0 c^2}\right)^5 \cdot < H > \quad (1)$$

where

$$< H >= \frac{1}{\theta} \cdot \int_0^{\theta} (\gamma\eta^2 + 2\alpha\eta\eta' + \beta\eta'^2) d\psi \quad (2)$$

θ is the deflecting angle of one magnet. α, β and γ are the Twiss-parameters and $\eta = (1 - \cos\psi)$ and $\eta' = \sin\psi$ are the matrix elements for dispersion and angular dispersion within the magnet, respectively. Obviously, there is a rapid increase of $\Delta\varepsilon$ with energy E, such that e.g. in MAMI the horizontal emittance for 99.9% of the beam is increased to 0.14 π·mm·mrad. The corresponding beam width is about 5 mm.

It is seen that the energy limit of the RTM scheme is roughly marked by MAMI.

3 HIGHER ORDER MICROTRONS

For higher energy, some weight saving philosophy for the magnets is required and the value of $< H >$ has to be reduced. Both of it may be achieved by reducing the deflecting angle per magnet, thus generating "higher order" microtron schemes (fig. 3). The Bicyclotron, first proposed by O.A. Valdner was closer investigated by Kaiser [14], the Hexatron was proposed by Argonne National Lab. [15] and the Oktotron, using 8 magnets and 4 linacs, was proposed by Belovintsev et al. [16], all for the lower GeV range. The resonance condition mentioned at the beginning closely links the main parameters of such machines. It is obtained from a simple analysis of the orbit geometry as:

scheme	θ [deg]	N	ΔE_c [MeV]
RTM	180	1	5.73
Bicyclotron	90	2	31.5
Hexatron	60	3	99.3
Oktotron	45	4	230
	12	15	11774

Table 2: microtron parameters

$$\nu\lambda = \frac{2}{ec} \cdot \frac{\Delta E_c}{B} \cdot (\theta - \sin\theta) \quad (3)$$

where B is the flux density in the magnets. The energy gain ΔE_c required per revolution increases very rapidly with θ decreasing, as is demonstrated in table 2 using λ = 12 cm and B = 1 Tesla, $N = \pi/\theta$ being the number of magnet pairs.

As a rough estimate, $< H >$ is inversely proportional to N^3 [17]. Thus, the expression (1) is kept constant if N is raised proportional to E, i.e. the number N represents roughly also the output energy limit in GeV. On the other hand, it is seen from the table that the energy gain per revolution might even surpass the output energy above 10 GeV, thus spoiling the recirculation concept.

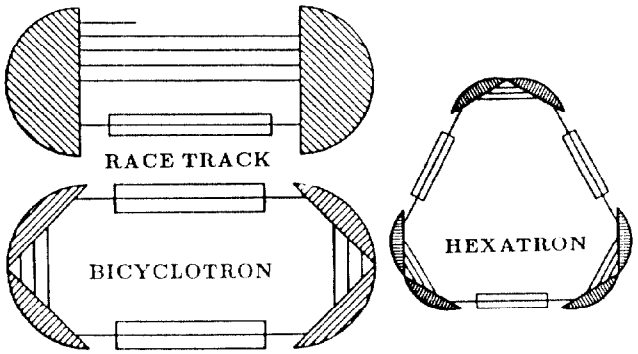

Figure 3: microtron schemes

Figure 4: Scheme of a bending magnet. The dotted lines indicate the blocks.

4 POLYTRONS

This may be cured by allowing more than one magnet pair between adjacent linacs. Be N_L the number of linacs installed, then N/N_L is the number of magnet pairs between adjacent linacs. In that case, eq. (3) is to be rewritten as

$$\nu\lambda = \frac{2}{ec} \cdot \frac{\Delta E_c}{B} \cdot \frac{N}{N_L} \cdot (\theta - \sin\theta) \qquad (4)$$

Thus, the installed energy gain from eq. (3) is to be divided by the number of magnet pairs between linacs. This scheme, referred to as "Polytron", may be used as a recycling accelerator beyond 10 GeV.

Detailed design considerations and several examples for 15 GeV output energy are given in [17].

4.1 Magnet system

Typically, in a polytron the bending angle per magnet is small. Thus, the pole face edges have to be of a stair like shape to allow adequate beam optics, as shown schematically in fig. 4. Further, the poles are much longer as compared to their width. Therefore, it would be advisable to compose each magnet from several, essentially identical iron blocks, each block forming a single stair. This also makes adjustment easier and allows individual trimming of each stair by means of small trim coils. The blocks would be stacked together (leaving a few mm air gap in order to avoid a magnetic short for the trimcoil), and would be excited by one common "coil" consisting of one single lead.

Computations using the PROFI code showed that under realistic conditions the beams passing a magnet outside

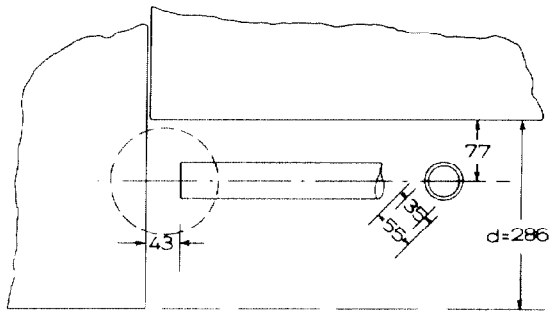

Figure 5: Detail of a typical polytron staircase magnet: transition from stair to shielding tube, measures in mm. Flux density is 0.53 Tesla, gap width is 60 mm.

parallel to the pole edge can be shielded very effectively from the fringe field by simple iron tubes and that the field distribution between stair and iron tube (dashed circle) gives quite satisfactory beam optics in the arrangement of fig. 5.

A quadrupole triplett or quintett between the magnets of a pair serves for dispersion matching such that the dispersion vanishes on either end of a pair ("Brown-System").

4.2 Output energy stability

As pointed out elsewhere in more detail [18], a very effective stabilisation of the output energy of a recirculating accelerator occurs if the machine is tuned such that there is an integer number of synchrotron oscillations during acceleration. The effect can be understood as an imaging of the input emittance onto the output. Fig. 6 shows two examples for the effectiveness of this stabilisation, taking account also for the tune shift caused by synchrotron radiation loss. In both cases a polytron with five revolutions is assumed, using three linacs which are connected by bends consisting of eight magnet pairs each. Operating frequency is 1.5 GHz. The two examples refer to 15 and 30 GeV output energy respectively, thus energy gains per linac of 1 and 2 GeV and flux densities of 0.299 and 0.598 Tesla respectively. In both cases, the longitudinal tune is chosen such that two phase oscillations occur during acceleration. Amplitude and phase are assumed to jitter by 0.6 % and 0.5 deg bin respectively, uncorrelated in all three linacs. At 15 GeV, it is seen from the figure that the resulting output energy jitter is suppressed to about 0.02 % bin. At 30 GeV, the stabilisation suffers noticeably from the tune shift by radiation loss. Yet the jitter is still suppressed by an order of magnitude at the output.

4.3 Monitoring of longitudinal dispersion

For any recirculation system – isochronous or not – it is essential to know the actual longitudinal tune. Therefore, a method should be available by which the longitudinal tune can be checked. It should be realized that the powerful diagnostics of storage rings are not applicable to a

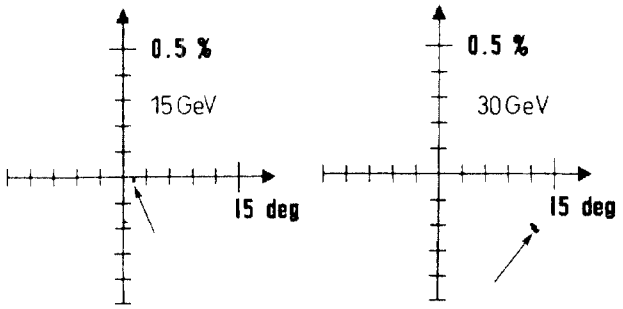

Figure 6: Jitter of energy and phase at the output of a polytron, caused by jitter of accelerating field of 0.6 % in amplitude and 0.5 deg in phase. The shift off the origin is due to synchrotron radiation loss, most of which is compensated automatically by the phase shift.

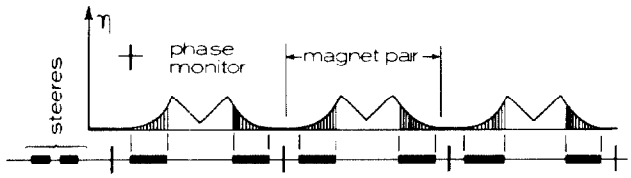

Figure 7: Polytron type lattice with instrumentation for longitudinal tune check.

recirculator because they are based on multiple passage of one and the same ring.

There is, however, an elegant possibility to check the proper tune of a non isochronous lattice consisting of pairs of magnets on either side of which the dispersion vanishes identically ("polytron type") [19].

The transfer matrix in the deflecting plane of any beam guiding system may be written as

$$\begin{pmatrix} c & s & 0 & \eta \\ c' & s' & 0 & \eta' \\ -\int \frac{c}{\rho} & -\int \frac{s}{\rho} & 1 & -\int \frac{\eta}{\rho} \\ 0 & 0 & 0 & 1 \end{pmatrix}$$

where $\eta = s \cdot \int(c/\rho) - c \cdot \int(s/\rho)$ and $\eta' = s' \cdot \int(c/\rho) - c' \cdot \int(s/\rho)$ are dispersion and angular dispersion respectively.

It is seen that vanishing of both coupling terms $-\int(c/\rho)$ and $-\int(s/\rho)$ is necessary and sufficient for $\eta = \eta' = 0$. Thus, if the lattice of fig. 7 is tuned such that the bunch phases between cells are not affected by any steering in front of the lattice, then there is zero dispersion between the cells, meaning that $\eta = \rho \cdot (1 - \cos\theta)$ in both magnets, so that the longitudinal dispersion is given by $-2 \cdot \int(\eta/\rho) = -2 \cdot \rho(\theta - \sin\theta)$, as required. An estimation shows [19] that, with a few μA of beam current and with typical polytron parameters, the method is sufficiently sensitive to adjust longitudinal dispersion to within about 1 % of its nominal value. Note that one single monitor set is used in common for all revolutions. To accomplish tuning for each revolution, the polytron would be filled "head to tail" over one revolution.

5 ACKNOWLEDGEMENTS

The kind support of the Deutsche Forschungsgemeinschaft and the Institut für Kernphysik of Mainz University is gratefully acknowledged. I particularly appreciate the helpful work of Mrs. U. Ludwig-Mertin who did the PROFI computations and finally helped in preparing the manuscript.

6 REFERENCES

[1] H. Herminghaus et al., "The Design of a Cascaded 800 MeV Normal Conducting CW Race Track Microtron", Nucl. Instr. and Meth. 138 (1976) p.1

[2] H. Herminghaus et al., "Status Report on the Normal Conducting CW Race Track Microtron Cascade MAMI", IEEE NS 30, No.4, Aug. 1983, p. 3274

[3] H. Herminghaus et al., "First Operation of the 850 MeV CW Electron Accelerator MAMI", Proc. Conf. LINAC 90, Rep. Los Alamos Nat. Lab. LA-12004-C, p. 362

[4] K.H. Kaiser et al., "Four Years of Operation of the 180 MeV Electron Accelerator MAMI A", Proc. Conf. EPAC 1988, Rome, ISBN 9971-50-642-4, p. 371

[5] H. Braun et al., "The Gun/Chopper System for the Mainz Microtron", ibid. p. 997

[6] H. Euteneuer et al., "Fast Longitudinal Phase Space Diagnostics for the Injector Linac of MAMI", ibid. p. 1149

[7] H. Euteneuer et al., "The Injector Linac of the Mainz Microtron", ibid. p. 550

[8] W. Hartmann et al., "Source of Polarized Electrons", ibid.p.1335

[9] H. Herminghaus et al., "The Reversing Magnets of the 850 MeV Stage of MAMI", ibid. p. 1151

[10] H.J. Kreidel, "Computer Aided Beam Diagnostics and Automatic Matching on the Mainz Microtron", ibid. p. 1205

[11] H. Schöler, H. Euteneuer, "Corrosion of Copper by Deionized Water", ibid. p. 1067

[12] H. Herminghaus, "The Mainz Microtron-Operating Experience and Upgrade Progress", Proc. Conf. LINAC 88, Williamsburg, CEBAF-Report-89-001, p. 247

[13] H. Euteneuer et al., "Experience with the 855 MeV RTM-Cascade MAMI", this conference.

[14] K.H. Kaiser, "A Possible Magnet Field Configuration for a CW Electron Accelerator in the GeV region", Proc. of the Conf. on Future Possibilities for Electron Accelerators, 1979, Charlottesville, VA

[15] H.E. Jackson et al., Argonne Publication ANL-82-83(1982)

[16] K.A. Belovintsev et al., Preprint No. 88, Lebedev Institute, Moscow 1984

[17] H. Herminghaus, "The Polytron as a CW Electron Accelerator in the 10 GeV Range", Nucl. Instr. and Meth. A 305 (1991), p. 1

[18] H. Herminghaus, "On the Inherent Stability of Non Isochronous Recirculating Accelerators", Nucl. Instr. and Meth. A, (1992) in print

[19] H. Herminghaus, "Beam Monitoring and Optics Analysis in Recirculators", Institut f. Kernphysik Univ. Mainz, Int. note MAMI 7/91.